RAI Volume 3, Chapter 2.2.1.2.1, Sixth Set, Number 5:

Provide an explanation of how rock blocks at the drift interface maintain cohesion after failure when the modeled stress-strain curve (DOE, 2009, RAI-3, Figure 1-4) indicates a brittle mode of rock failure should occur. Additionally, clarify how blocks in the UDEC-Voronoi model remain in place if the supporting contacts between the blocks have failed.

Basis: DOE concluded the UDEC-Voronoi model shows a more brittle response compared to the stress-strain test on Topopah Spring lower lithophysal tuff (DOE, 2009, RAI-3 and RAI-5). Additionally, the modeled post-peak curves presented in BSC (2004, section 7.6.4) are nearly vertical, and represent a near-brittle mode of deformation (e.g., Jaeger and Cook, 1979). Thus, the near-vertical slope of the post-peak portion of the modeled stress-strain curves suggests that, after failure, the remaining rock strength should be negligible, consistent with a brittle failure mechanism. Additionally, in DOE (2009, RAI-1, Figure 1-3), the UDEC model appears to allow some blocks at the drift wall to remain in place after the supporting contacts between the blocks have failed. This result appears inconsistent with the modeling approach, in which blocks supported by failed contacts should fall from the drift wall.

1. RESPONSE

1.1 MACROSCOPIC RESPONSE OF A VORONOI BLOCK MODEL

The macroscopic response of a Voronoi block model is determined primarily by the collective response of the numerous contacts between individual Voronoi blocks. The contacts between individual blocks represent small, pre-existing joints that can fail under mechanical loading. The contacts represent the "weak links" that control the overall strength of the rock mass because the shear or tensile stress and associated energy required to fail an individual contact are typically much less than the stress and energy required to drive a new fracture through intact blocks. The failure of an individual contact has negligible impact on the strength of the overall rock mass as long as most other contacts remain intact. But when failed contacts coalesce into a discrete fracture on the size scale of the rock mass, failure occurs in the macroscopic sense, even though many contacts remain intact away from the failed region. Stated differently, slippage along a discrete fracture can result in failure of a rock mass, although the rock mass retains some strength from two mechanisms. First, energy is required to overcome friction and drive slippage along the discrete fracture if a confining stress is present. Second, the unfailed rock surrounding the fracture retains its original strength across the intact contacts between individual Voronoi blocks. It follows that a rock mass can maintain some cohesion, even after failure, because many contacts remain intact after macroscopic failure is observed. A detailed description of the mechanical properties of the contacts/joints, including their cohesion, tensile strength, and frictional resistance, can be found in Section 7.6.4 of *Drift Degradation Analysis* (BSC 2004).

1.1.1 Response of Individual Contacts

The brittle macroscopic response of the Voronoi block model, manifested during calibration simulations (BSC 2004, Section 7.6.4 and Figure 7-20), is caused by the failure of the contacts between individual blocks. Failure occurs when the shear stress, or tensile stress at a particular contact, exceeds its given limit. Failure of a contact results in the instantaneous loss of both cohesion and tensile strength, although a failed contact retains some residual strength from frictional resistance to sliding when the normal stress across the contact is compressive. This frictional resistance means that the local response after contact failure is not perfectly brittle when there is compressive stress in the contact.

1.1.2 Collective Response of the Contacts

The overall response of the Voronoi block model is the result of the interaction of a large number of blocks and joints. This macroscopic response produces the stress-strain curves observed in Universal Distinct Element Code (UDEC) calculations using synthetic core models. The stress state inside the Voronoi block model for a synthetic core is inhomogeneous (i.e., the stresses vary between the blocks and the contacts), even under uniform external mechanical loading, because of the geometric irregularities between blocks. As a consequence, not all contacts break when the peak strength is reached. Instead, the first fracturing or contact breakage occurs at a stress level below the peak strength (i.e., the crack initiation stress). As the load increases, the number of broken contacts, as well as the rate of contact failure, increases. Just before the peak strength is reached, the failed contacts start coalescing and forming macro fractures. This description of model response is similar to the failure process inferred from monitoring acoustic emissions during laboratory tests (e.g., Diederichs 2003, Figure 8). Acoustic emissions, indicating formation of micro cracks, start at the load levels which are typically at 40% of the unconfined strength. The cracking rate, as recorded by the acoustic emissions, is largest as the load approaches the rock strength.

Even in the post-peak state, Figure 1 demonstrates that the rock within the synthetic model has not completely disintegrated after formation of discrete macro fractures. Although stress can decrease to 50% of the peak stress in the post-fracture state, as shown by the end of the blue line in Figure 1, the material is not perfectly brittle because the post-peak slope of the blue stress-strain curve remains finite. This behavior is consistent with Figure 2, which compares the geometry and cracking of the UDEC Voronoi block model with a test core at the end of an unconfined compression test. Figure 2 shows that, at the end of testing, there is still a large volume of rock that is unfractured for both the Voronoi block model and for the test core. Although Figures 1 and 2 show that the macroscopic response of the core after failure is softening in a brittle manner and losing a significant portion of its apparent (macroscopic) cohesion, large volumes of rock internally maintain their intact cohesion. The term “softening” describes degradation of strength as a function of deformation after the peak-strength of material has been reached (BSC 2004, Section 7.4.1).

1.1.3 Post-Failure Response of the Rock Mass

The post-failure response of the Voronoi block model is not perfectly brittle because of the presence of unfractured rock mass and because of the frictional resistance to slippage in the failed contacts and macro fracture(s). These features produce a finite softening rate and some residual strength after failure of the core, as shown by the finite slope of the blue curve in Figure 1 after peak stress. Stated differently, the UDEC Voronoi block model under unconfined compression has some small but finite ductility. At any point of the stress-strain curve, even on the softening part, it is necessary to provide additional energy to continue deformation of the sample.

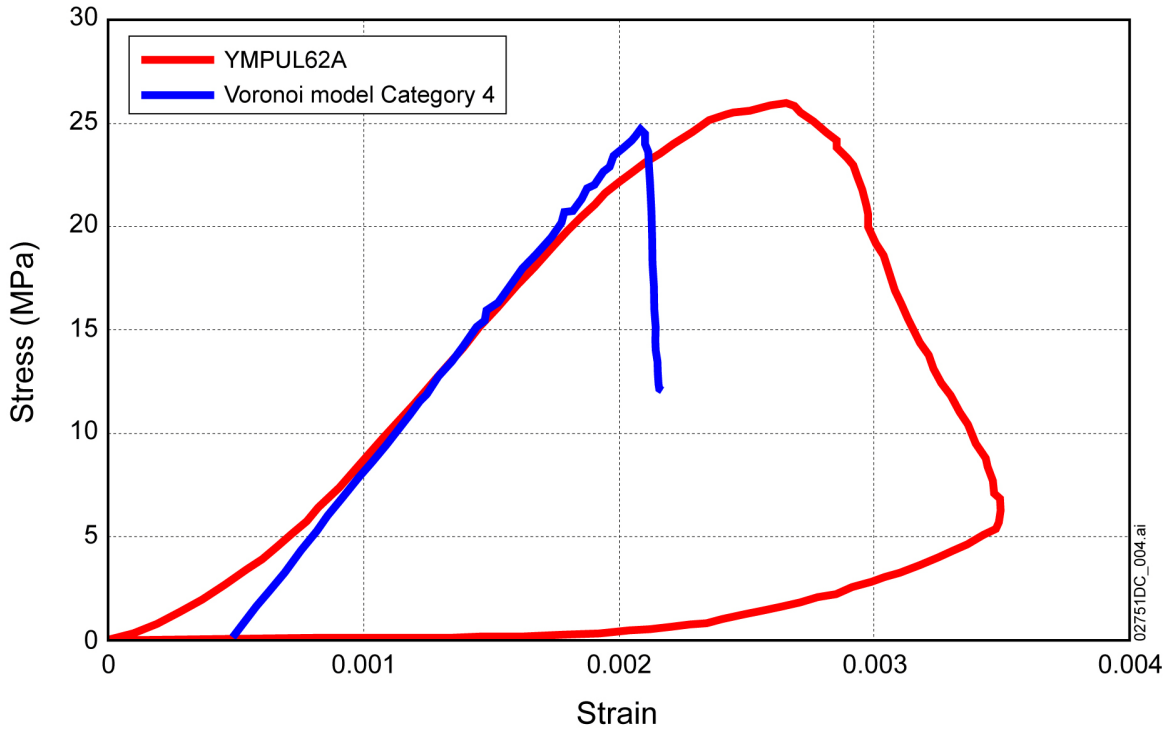

NOTE: Laboratory results are in red; numerical results are in blue. The red line returns to origin because at the end of loading part of experiment, when the strength decreased to approximately 5 MPa, the sample was completely unloaded.

Figure 1. Comparison of Stress-Strain Curves Measured in the Laboratory on a Lithophysal Sample and Obtained by Voronoi Block Model Calibration

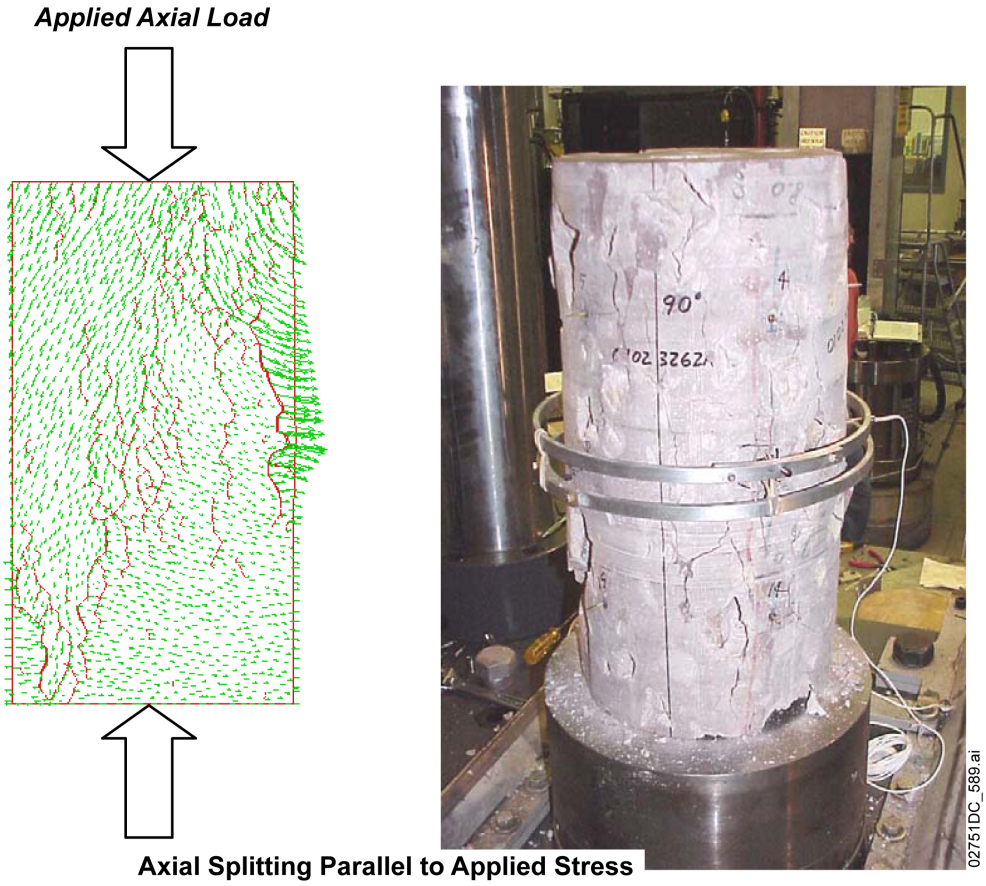

Source: BSC 2004, Figure 7-23.

Figure 2. UDEC Discontinuum Model of Failure of Lithophysal Tuff Specimen under Uniaxial Compression

Perfectly brittle (or very close to perfectly brittle) materials fail violently, with a sudden release of energy at peak strength, even when loaded by very stiff loading frames. Typically, rocks with perfectly brittle failure disintegrate into very small pieces. That was certainly not the case for the laboratory testing of lithophysal rock cores (see Figure 2), and the UDEC Voronoi block model behaves in a similar manner to the laboratory tests. When it yields, the UDEC model loses macroscopic cohesion, but failure does not result in complete disintegration with a complete loss of cohesion at every contact between the Voronoi blocks. Although the macroscopic strength of the sample during the softening phase can drop to a small fraction of its intact strength, large volumes (pieces) of rock in the core are undamaged (i.e., maintain their initial cohesion). The Voronoi block model does not represent perfectly brittle material response, consistent with the laboratory testing.

Because the lithophysal tuff is not perfectly brittle, it does not disintegrate into small fragments, and the test core and model reach equilibrium under the action of gravity, completely unsupported and without any significant piece of rock falling off the sample. No pieces of rock are unstable under gravity because, in this particular test, the fracture pattern does not form any

loose blocks along the free boundaries on the sides of the core. A similar observation is valid for the walls of the drift, as explained in the next section.

1.2 STABILITY OF BLOCKS NEAR THE DRIFT BOUNDARY

Fractures will develop near the drift boundary under increasing mechanical loads. Initially, the fractures would be relatively random at lower loads, but with increasing stress, the number of fractures will increase and the existing fractures will extend in length. This fracturing causes local yielding of the fractured rock mass and a redistribution of stresses from the fractured region to the regions away from the excavation where the rock is more confined and stronger. The failed rock mass does not completely lose its cohesive strength when it yields because of this stress distribution and because the rock is not perfectly brittle.

Near the drift boundary, the fractures can potentially detach volumes of rock from the rock mass, resulting in loose rock blocks. However, as will be demonstrated in the examples below, fracturing will not result in rockfall as long as there are unfractured segments, or rock bridges, connecting volumes of rock outlined by fractures with the intact rock mass. As shown by simple stability analyses (Sections 1.2.1 and 1.2.2) and illustrated in Figures 3 through 8, on the scale of the emplacement drift, the strength of rock bridges even 1 cm in length is sufficient to support the weight of potentially loose blocks.

Even if the internal stresses fracture the rock mass in such a way as to form completely detached rock blocks (i.e., outlined by fractures), the frictional resistance across failed contacts may be sufficient to keep blocks in place under the action of gravity.

These processes are illustrated in Figure 3, and are also presented in Figure 1-3 of the response to RAI 3.2.2.1.2.1-001. Figure 3 presents the detailed geometry of the drift crown blocks after 100 years of heating, including locations of the failed contacts and principal stress tensors. Two destressed zones on the drift boundary, almost completely outlined by failed contacts, are indicated in the figure.

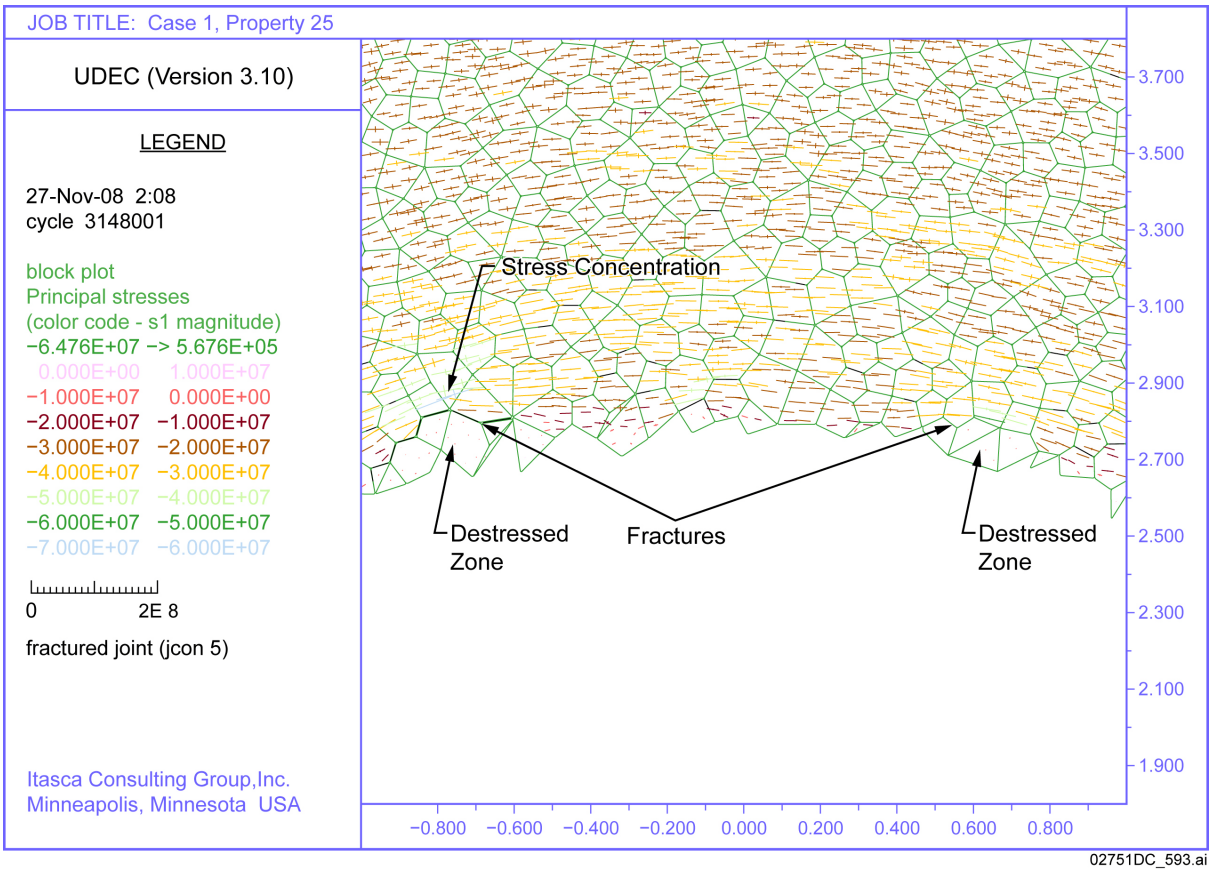

Source: Figure 1-3 of response to RAI 3.2.2.1.2.1-001.

NOTE: Locations where contacts between the blocks have failed are indicated by black lines (see two black lines in destressed zones). Compressive stresses are negative. Distance is in meters. The x-axis is horizontal to the right; the y-axis is vertical, upward.

Figure 3. Detail of Drift Crown, with Stress Tensor Field (Pa) Colored by Magnitude of the Major Principal Stress, after 100 Years of Heating as Predicted by the Model with 0.1-m Voronoi Block Size

1.2.1 Stability and Force Analysis for Left Destressed Zone

The detail of the block geometry and fracturing around the left destressed zone in Figure 3 is shown in Figure 4. On the scale of Figure 4, it is clear that fractures do not completely detach the left destressed zone at the drift boundary because there is still an unfractured segment (rock bridge) connecting the potentially unstable zone to the remaining rock mass. This unfractured segment represents a partly failed contact, which is possible because UDEC uses a discretized representation for contact failure. In addition, Figure 5 shows that the potentially unstable zone (circled detail in Figure 4) is also supported on the right side at a frictional point contact.

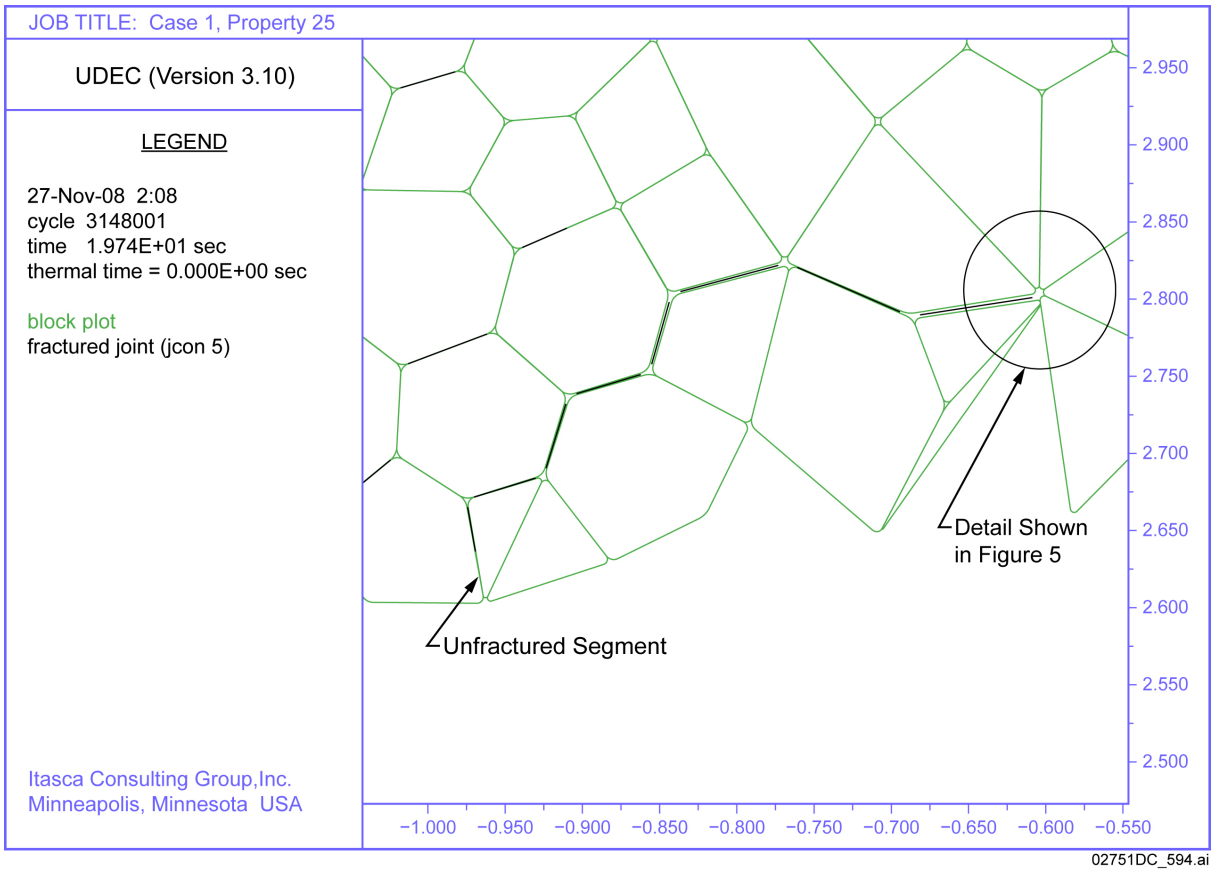

NOTE: Locations of micro-cracks or failed contacts between blocks are indicated by black lines. Distance is in meters. The x-axis is horizontal to the right; the y-axis is vertical, upward.

Figure 4. Detail of Block Geometry and Cracking around the Left Destressed Zone from Figure 3

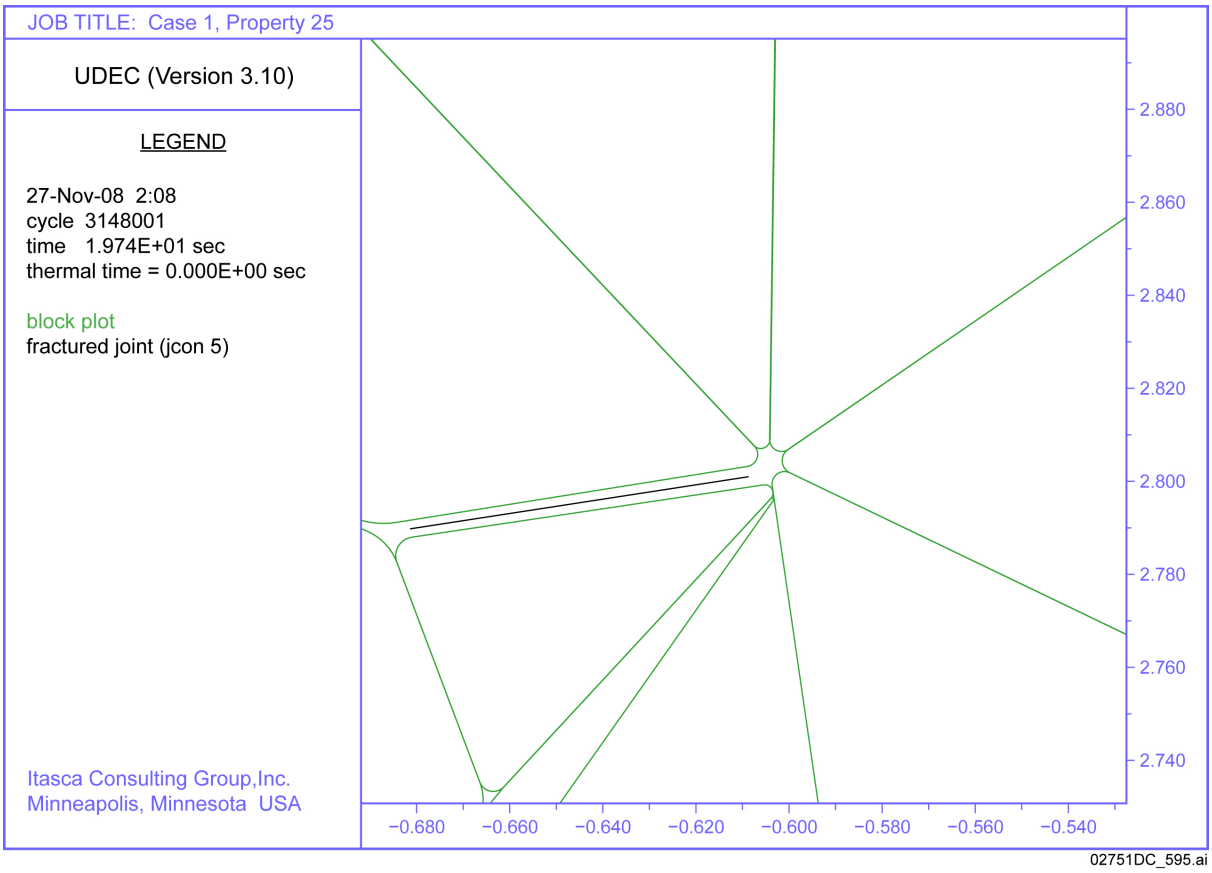

NOTE: Locations of micro-cracks or failed contacts between blocks are indicated by black lines. Distance is in meters. The x-axis is horizontal to the right; the y-axis is vertical, upward.

Figure 5. Detail of Block Geometry and Cracking around the Left Destressed Zone Indicated in Figure 4

A simple stability analysis for the potentially unstable zone of blocks outlined in Figure 4 is presented here. The mass of each Voronoi block within the potentially unstable block and the total mass of the zone are listed in Table 1. The weight of blocks in the zone is (80.17 kg)(9.81 m/s^2) = 786 N ~ 0.8 kN. The uncracked length of the contact is 2.91 cm, and considering cohesion of 14.3 MPa and tensile strength of 5.67 MPa of the joints, the maximum normal and shear forces that can be carried by the unfractured bridge is (5.67×10^6 Pa)(0.0291 m)(1 m) = 1.65×10^5 N = 165 kN and (14.3×10^6 Pa)(0.0291 m)(1 m) = 4.16×10^5 N = 416 kN, respectively. (The factor of 1 meter in these equations represents the unit depth of the two-dimensional UDEC model.) Thus, the tensile strength of the bridge exceeds the weight of the zone by more than a factor of 200 and the cohesion of the bridge exceeds the weight of the zone by more than a factor of 500. The bridge (alone) is capable of carrying the potentially unstable zone, even if it acts as a cantilever (i.e., has support only on one side). However, in this case, the potentially unstable zone is actually supported on two sides.

Table 1. Mass of Blocks in Figure 4

Block ID	Mass (kg)
21620090	3.802
16681872	6.109
16118251	22
18718928	11.8
17176873	28.5
16968129	5.46
17139413	2.5
Sum	80.17

It is also instructive to perform an analysis of the contact forces on the potentially unstable zone. All forces acting between the zone and surrounding rock mass are indicated in Figure 6. (The forces are shown as normal and shear force relative to the contact orientation.) The only additional force acting on the block in the negative y-direction is its own weight, which is 0.8 kN (based on the sum of masses from Table 1). The forces acting in the contacts at two ends projected on the x- and y-coordinate axes are listed in Table 2. Table 2 shows that the contact horizontal forces are in equilibrium (i.e., + 77.0 kN compared to −77.0 kN) because they sum to zero. Also, the forces acting in the vertical direction are almost in equilibrium. The vertical force is given by the downward force from the rock mass on the zone, 40.3 kN from Table 2, plus the weight of the block, 0.8 kN, for a total downward force of (−40.3 kN) + (−0.8 kN) = −41.1 kN, which is practically in equilibrium with the upward force, +41.2 kN. The rock mass is not in perfect equilibrium because of numerical roundoff caused by small elastic waves that exist in UDEC's solution for the dynamic equations of motion.

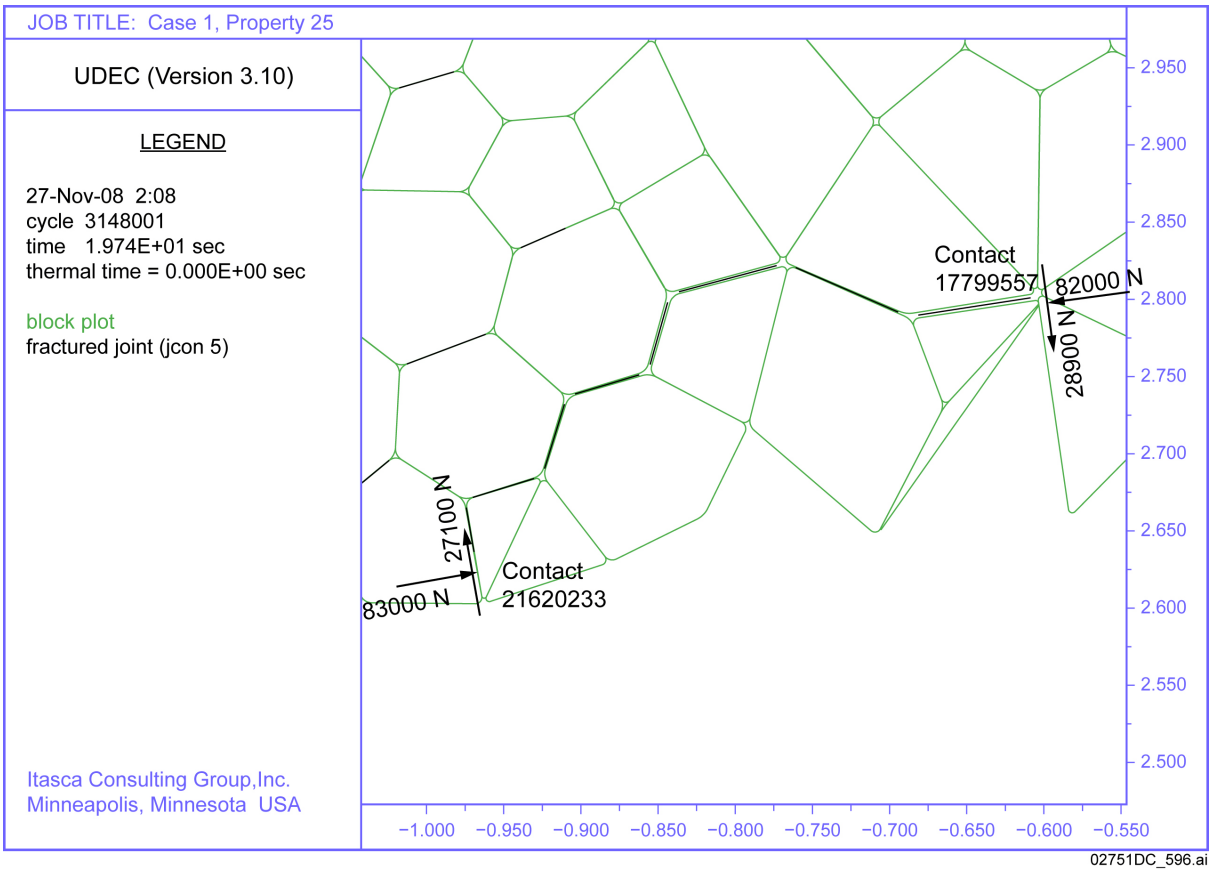

NOTE: Locations of micro-cracks, or locations where contacts between the blocks have failed, are indicated by black lines. Distance is in meters and force is in Newtons. The x-axis is horizontal to the right; the y-axis is vertical, upward.

Figure 6. Detail of Block Geometry and Cracking around the Left Destressed Zone from Figure 3

Table 2. Balance of Forces Acting on the Destressed Zone in Figure 6

Contact	Angle (°)	Horizontal force (kN)	Vertical force (kN)
21620233	79.95	77.0	41.2
17799557	81.76	−77.0	−40.3

1.2.2 Stability Analysis for Right Destressed Zone

The detail of the block geometry and fracturing around the right destressed zone from Figure 3 is shown in Figure 7. Again, there is an unfractured rock bridge that prevents the portion of the model outlined by fractures from becoming unstable. In this case, the potentially unstable block acts as a cantilever. However, a simple analysis of block weight and bridge strength clearly illustrates that the rock bridge strength is sufficient to carry the weight of potentially unstable rock in this case.

The uncracked length of contact, which represents the rock bridge, is 1.90 cm, and considering cohesion of 14.3 MPa and tensile strength of 5.67 MPa, the maximum normal and shear forces that can be carried by unfractured bridge are $(5.67 \times 10^6$ Pa$)(0.0190$ m$)(1$ m$) = 1.08 \times 10^5$ N = 108 kN and $(14.3 \times 10^6$ Pa$)(0.0190$ m$)(1$ m$) = 2.72 \times 10^5$ N = 272 kN, respectively. Thus, the strength of the bridge considerably exceeds the weight of the destressed zone, which is (53.504 kg)(9.81 m/s^2) = 525 N ~ 0.53 kN (Table 3).

A balance of force calculation for the contacts has not been performed for the right destressed zone because the cantilever geometry generates an internal force in the neck of the rock bridge that balances the action of gravity on the distressed zone, but there is not a balance between contact forces on both sides of the zone.

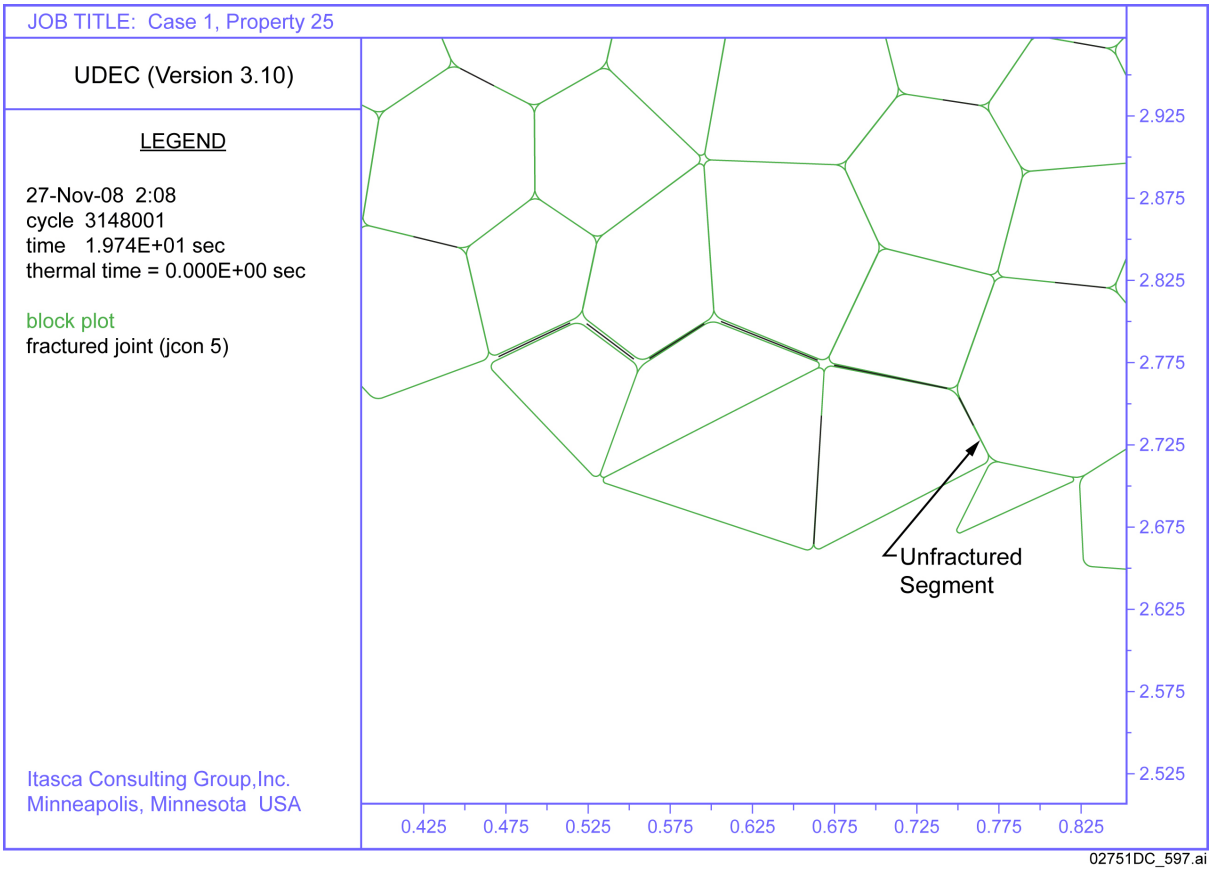

NOTE: Locations of micro-cracks, or locations where contacts between the blocks have failed, are indicated by black lines. Distance is in meters. The x-axis is horizontal to the right; the y-axis is vertical, upward.

Figure 7. Detail of Block Geometry and Cracking around the Right Destressed Zone from Figure 3

Table 3. Mass of Blocks in Figure 7

Block ID	Mass (kg)
18342239	9.584
16750482	11.64
20819476	16.27
16839203	16.01
Sum	53.504

1.2.3 Time Dependence of Drift Wall Stability

Figure 3 corresponds to the condition of the destressed zone after 100 years of heating. After 1,000 years of heating, the left distressed zone is still attached to the drift wall, as shown in Figure 8. The right destressed zone eventually detaches from the drift wall under long-term thermal heating, and thus is no longer shown in Figure 8.

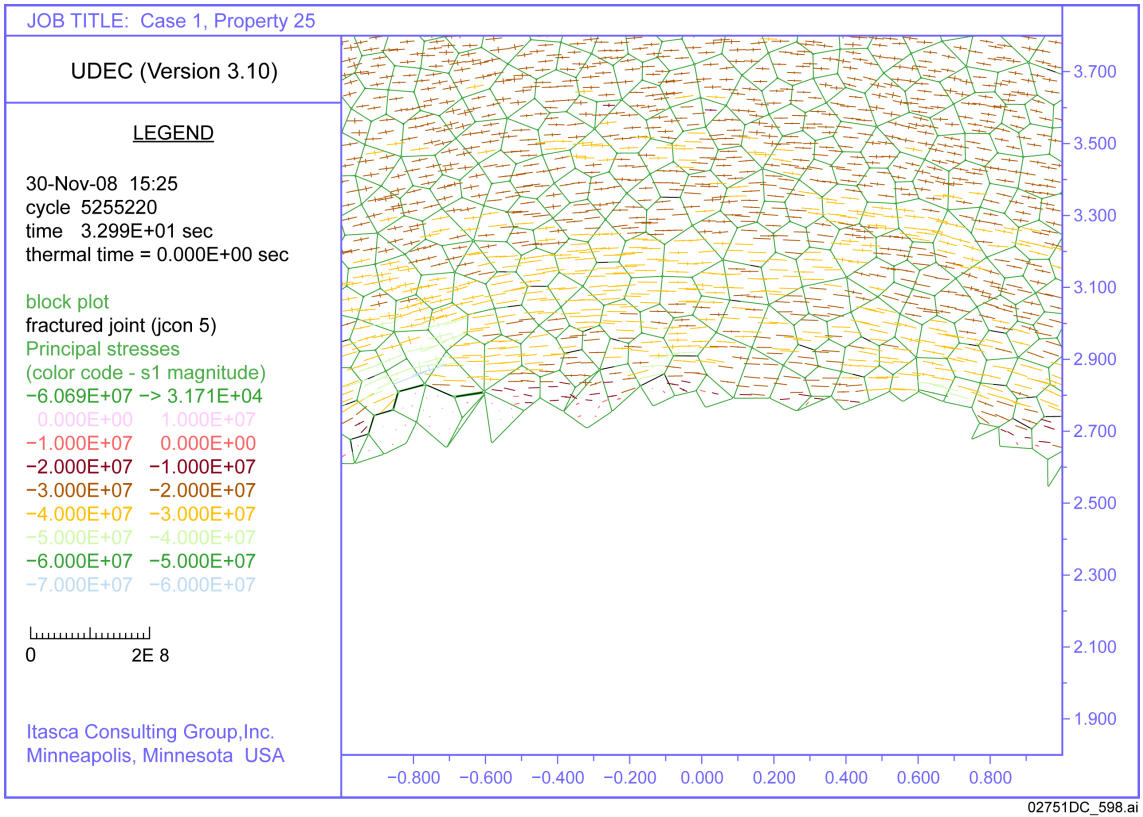

NOTE: Locations of micro-cracks, or locations where contacts between the blocks have failed, are indicated by black lines. Compressive stresses are negative and distance is in meters. The x-axis is horizontal to the right; the y-axis is vertical, upward.

Figure 8. Detail of Drift Crown, with Stress Tensor Field (Pa) Colored by Magnitude of the Major Principal Stress, after 1,000 Years of Heating as Predicted by the Model with 0.1-m Voronoi Block Size

1.3 SUMMARY

The macroscopic response of a Voronoi block model is determined primarily by the collective response of the numerous contacts between individual Voronoi blocks. Failure occurs when failed contacts coalesce into a discrete fracture on the size scale of the rock mass, although the rock mass retains significant strength from two mechanisms. First, energy is still required to overcome frictional resistance for motion along the failed contacts. Second, the unfailed rock surrounding the fracture retains some cohesion (i.e., does not disintegrate), even after failure, because many contacts throughout the rock mass remain intact.

The brittle macroscopic response of the Voronoi block model manifested during calibration simulations for synthetic cores is caused by the failure of the contacts between individual blocks. Failure occurs when the shear stress or tensile stress at a particular contact exceeds its given limit. Failure of a contact results in the instantaneous loss of both cohesion and tensile strength, although a failed contact retains some residual strength from frictional resistance to sliding when the normal stress across the contact is compressive.

Typically, rocks with perfectly brittle failure disintegrate into small fragments. This behavior is not observed during laboratory testing of lithophysal rock cores, and is not observed in the UDEC calibration runs for synthetic rock cores. Failure in the UDEC model does not result in complete disintegration with a complete loss of cohesion at most contacts between the Voronoi blocks. Although the macroscopic strength of the sample during the softening phase can drop to a small fraction of its intact strength, large volumes (pieces) of rock in the core are undamaged (i.e., maintain their initial cohesion). The Voronoi block model does not represent perfectly brittle material response, consistent with the laboratory testing. Therefore, the post-failure remaining rock strength is not negligible, as was suggested in the Basis for the RAI. Rather, the remaining rock strength is found, both experimentally and in the UDEC Voronoi modeling approach, to be more than sufficient to keep the fractured blocks in place.

Near the walls of a drift, fractures can potentially detach volumes of rock from the rock mass, resulting in rockfall. However, fracturing will not result in rockfall as long as there are unfractured segments, or rock bridges, connecting volumes of rock outlined by fractures with the intact rock mass. Even if the internal stresses fracture the rock mass in such a way as to form completely detached rock blocks (i.e., outlined by fractures), the frictional resistance across failed contacts may be sufficient to keep blocks in place under the action of gravity. This argument is not inconsistent with the modeling approach because formation of fractures near the drift walls does not necessarily result in a rockfall.

These processes are illustrated for two destressed zones from a UDEC calculation of drift stability in this RAI response. These examples show that even short rock bridges, on the order of 1 cm in length, are sufficient to stabilize a destressed zone of rock near the drift wall under gravitational loads.

2. COMMITMENTS TO NRC

None.

3. DESCRIPTION OF PROPOSED LA CHANGE

None.

4. REFERENCES

BSC (Bechtel SAIC Company) 2004. *Drift Degradation Analysis*. ANL-EBS-MD-000027 REV 03. Las Vegas, Nevada: Bechtel SAIC Company. DOC.20040915.0010.

Diederichs, M.S. 2007. "The 2003 Canadian Geotechnical Colloquium: Mechanistic Interpretation and Practical Application of Damage and Spalling Prediction Criteria for Deep Tunnelling." *Canadian Geotechnical Journal, 44*, 1082-1116. Ottawa, Ontario, Canada: National Research Council Canada.